ELSEVIER

Journal of Hepatology 46 (2007) 142–150

Journal of Hepatology

www.elsevier.com/locate/jhep

Fibrogenic cell fate during fibrotic tissue remodelling observed in rat and human cultured liver slices

Christelle Guyot[1,2], Chantal Combe[1,2], Charles Balabaud[1,3], Paulette Bioulac-Sage[1,4], Alexis Desmoulière[1,2,5,*]

[1]*INSERM, E0362, Université Victor Segalen Bordeaux 2, Bordeaux F-33076, France*
[2]*IFR 66, Bordeaux F-33076, France*
[3]*CHU Bordeaux, Hôpital Saint-André, Service d'Hépatologie-Gastroentérologie, Bordeaux F-33075, France*
[4]*CHU Bordeaux, Hôpital Pellegrin, Service d'Anatomie Pathologique, Bordeaux F-33076, France*
[5]*Département de Physiologie, Faculté de Pharmacie, Université de Limoges, Limoges F-87025, France*

***Background/Aims*: Fibrotic liver remodelling was studied in culture of precision-cut liver slices (PCLS) derived from fibrotic liver.**

***Methods*: Fibrosis was induced in rats by carbon tetrachloride (CCl_4) treatment or bile duct ligation. Human fibrotic livers were also used. PCLS were cultured for 6, 24, 48, or 72 h, and the expression of α-smooth muscle (SM) actin, platelet-derived growth factor (PDGF) receptor-β, and active caspase 3 was studied by immunohistochemistry.**

***Results*: Before culture, in CCl_4-treated or bile duct ligated animals, fibrosis was observed around centrolobular veins, or in portal zones, respectively. In PCLS derived from CCl_4-treated animals, α-SM actin expression disappeared after 24 h in culture while PDGF receptor-β expression decreased progressively after 48 h. These changes were observed in absence of massive apoptosis. In PCLS derived from bile duct ligated animals, both α-SM actin and PDGF receptor-β expression decreased after 48 h in culture with a massive apoptosis. In PCLS derived from human fibrotic livers, α-SM actin expression was dramatically reduced after 48 h in culture.**

***Conclusions*: After CCl_4 treatment, a proportion of myofibroblasts derived from hepatic stellate cells seems to dedifferentiate while in bile duct ligation model, myofibroblasts derived from portal fibroblasts disappear by apoptosis, underlining the relevance of this model to evaluate the mechanisms involved in fibrotic liver remodelling.**

***Keywords*: Liver fibrosis; Myofibroblast; Apoptosis; α-Smooth muscle actin; Platelet-derived growth factor receptor-β; Tissue remodelling; Fibrosis reversibility**

1. Introduction

Fibrosis is defined as the excessive deposition of extracellular matrix in an organ, and is the main complication of chronic liver damage. Its endpoint is cirrhosis, which is responsible for significant morbidity and mortality. The accumulation of extracellular matrix observed in fibrosis and cirrhosis is due to the activation of fibrogenic cells, which acquire a myofibroblastic phenotype. Myofibroblasts are absent from normal liver. They are produced by the activation of precursor cells, such as hepatic stellate cells and portal fibroblasts (for review, see [1]). These fibrogenic cells are distributed differently in the hepatic lobule: hepatic stellate cells resemble pericytes and are located along the sinusoids, in the Disse space between the endothelium and the hepatocytes (for review, see [2]), whereas portal fibroblasts are embedded in the portal tract connective tissue around portal structures (vessels

Received 18 March 2006; received in revised form 24 August 2006; accepted 27 August 2006; available online 4 October 2006

* Corresponding author. Tel.: +33 555 43 5873; fax: +33 555 43 5801.

E-mail address: alexis.desmouliere@unilim.fr (A. Desmoulière).

0168-8278/$32.00
doi:10.1016/j.jhep.2006.08.013

and biliary structures) [3]. Differences have been reported between these two fibrogenic cell populations, in the mechanisms leading to myofibroblastic differentiation, activation and "deactivation", but confirmation is required (for review, see [1]). It is now accepted that liver fibrosis is reversible, whereas cirrhosis seems generally irreversible [4–6]. However, the mechanisms involved in fibrosis reversibility are poorly understood.

Precision-cut liver slices (PCLS) have been used for metabolic and toxicological studies on various liver cell types [7,8]. The PCLS culture model allows the maintenance of normal lobular architecture and of cell–cell interactions within their original matrix. It has been recently applied to the study of hepatic stellate cell activation [9,10], and we have used this model to study the effects of bile acids on biliary epithelial cell proliferation and portal fibroblast activation [11].

In this study, we took advantage of the PCLS model, using a reduced number of animals, to analyse the remodelling of rat fibrotic liver in which fibrosis was induced *in vivo* by carbon tetrachloride (CCl_4) treatment or bile duct ligation; in addition, we have also studied fibrotic liver remodelling in cultured PCLS derived from human fibrotic livers.

2. Materials and methods

2.1. Experimental animals and liver removal

Male Wistar rats (Charles River, St. Aubin-les-Elbeuf, France) were used. Six animals were used in each experimental group. In the first group, animals were given CCl_4 (Sigma, St. Quentin-Fallavier, France) three times per week (375 μl/kg of body weight in olive oil per os) [12] and sacrificed three weeks after the first CCl_4 treatment. In the second group, animals were subjected to common bile duct ligation [3] and sacrificed one week after bile duct ligation. Control animals were used in each case. All experiments were performed using accepted ethical guidelines.

Liver was perfused *in situ* with preoxygenated ice-cold Hanks' balanced salt solution (HBSS) (Invitrogen, Cergy Pontoise, France), supplemented with 5 mM glucose and 50 μg/ml gentamycin, via a plastic catheter placed in the portal vein. After 5 min perfusion, the liver was excised.

2.2. Human liver tissues

Large non-tumoral liver specimens were obtained from four patients (Table 1). After washing in preoxygenated ice-cold HBSS, containing glucose and gentamycin, tissue was processed for PCLS preparation. The procedures were in accordance with the European Guidelines for the use of human tissues.

2.3. Rat and human precision-cut liver slices (PCLS) preparation, culture, and processing

PCLS were prepared as previously described [11]. Briefly, tissue cores were performed using a motor-driven coring tool (8 mm diameter). Consecutive PCLS (250 μm-thick) were obtained using a Krumdieck tissue slicer (Alabama Corporation, Munford, AL, USA). PCLS were placed on a stainless-steel insert (Alabama Corporation) in an incubation vial containing culture medium. Vials were set on a roller platform, and gently agitated in a humidified incubator (Sanyo, Osaka, Japan) at 37 °C, with 5% CO_2 and 40% O_2. Slices were firstly incubated in Williams' E medium (Invitrogen) supplemented with 0.35 μM insulin (Sigma), 0.1 μM dexamethasone (Sigma) and 5% fetal calf serum (FCS; Dutscher, Brumath, France). After 2 h, this medium was replaced by Williams' E medium supplemented with insulin, dexamethasone and 1% FCS. PCLS were cultured for 6, 24, 48, or 72 h.

After culture, PCLS were routinely formalin-fixed and paraffin-embedded. Sections (4 μm-thick) were stained with hematoxylin-eosin for routine histology, with Sirius red to allow visualization of fibrosis, or processed for immunohistochemistry. Some PCLS were frozen in liquid nitrogen to study by gelatin zymography, the enzymatic activity of matrix metalloproteinase (MMP)-2 and MMP-9 [13]. In addition, small fragments (approximately 1 mm^3) of PCLS were fixed in 1.5% glutaraldehyde in 0.1 M Sörensen phosphate buffer (pH 7.4) and routinely processed for transmission electron microscopy. Ultra-thin sections were double-contrasted and observed under a Tecnai 12 biotwin transmission electron microscope (Philips, Heindhoven, The Netherlands).

2.4. Antibodies and immunohistochemistry

For immunohistochemistry, primary antibodies were used according to Table 2. Platelet-derived growth factor (PDGF) receptor-β is a well-known early marker of fibroblastic cell activation [18–20]. α-Smooth muscle (SM) actin is the typical marker of fully differentiated myofibroblastic cells [21]. Active caspase 3 has been extensively used to detect cell apoptosis. Vimentin is present in mesenchymal cells [22] and in proliferating ductular cells [23]. Osteopontin is expressed by biliary epithelial cells [24]. All these antibodies have been extensively used and their specificity has been clearly documented (see references in Table 2).

Table 1
Human pathological specimens

Patient	Sex/age	Aetiology	Histology of the non-tumoral liver
1	M/57	Transplantation for a decompensated alcoholic cirrhosis with hepatocellular carcinomas	Micro/macronodular cirrhosis with moderate inflammation
2	F/46	Transplantation for a decompensated alcoholic cirrhosis without hepatocellular carcinoma	Micronodular cirrhosis with mild inflammation
3	F/63	Right hepatectomy for a gallbladder adenocarcinoma	Chronic obstructive cholestasis with secondary biliary fibrosis; enlarged portal tracts with some porto–portal septa, loose connective tissue, ductular reaction and a polymorphous inflammation; in centrolobular zones, cholestatic hepatocytes (ballooned and clarified) with intracanalicular biliary thrombi
4	M/78	Left hepatectomy for intrahepatic cholangiocarcinoma with vascular and large bile duct spread	Severe obstructive cholestasis with large porto–portal fibrous septa, obvious ductular reaction, secondary sclerosing cholangitis and huge intracanalicular thrombi.

Table 2
Primary antibodies

Protein	Host	Provided by
Collagen type I	Rabbit	Novotec, Lyon, France [14]
Collagen type III	Rabbit	Novotec [14]
α-SM actin	Mouse	DakoCytomation, Trappes, France [15]
PDGF receptor-β	Rabbit	Santa Cruz Biotechnology, Santa Cruz, CA, USA [16]
Active caspase 3	Rabbit	R&D Systems, Minneapolis, MN, USA [17]
Vimentin	Mouse	DakoCytomation
Osteopontin	Goat	Sigma, St. Quentin-Fallavier, France
Ki67	Mouse	DakoCytomation

SM, smooth muscle; PDGF, platelet-derived growth factor.

Immunohistochemistry was essentially performed as previously described [11]. Immunostainings were examined with a Zeiss Axioplan 2 microscope (Carl Zeiss Microscopy, Jena, Germany). Images were acquired with an AxioCam camera by means of the AxioVision image processing and analysis system (Carl Zeiss Microscopy).

2.5. Quantitative image analysis and statistical analysis

Fibroblast activation (PDGF receptor-β and α-SM actin stainings) was evaluated by quantitative image analysis. Images were acquired with a digital microscope Coolscope (Nikon, Champigny-sur-Marne, France), and the stained areas were measured using a computer-assisted image analysis system (LUCIA, Nikon). For CCl_4-induced fibrosis model, quantification was performed in centrolobular areas whereas for common bile duct ligation-induced fibrosis model, quantification was performed in portal areas. Three independent PCLS preparations were used per model, and for each time point, two PCLS were quantified. The analysis was performed on 30 fields per PCLS section using the ×20 objective (0.138 mm^2/field), and stained area was expressed as percent of the field. In order to minimize inter-individual variations, data obtained by quantification were normalized. For normalization, each datum was expressed as a relative variation rate (in percent) computed from the mean value obtained in non-cultured PCLS, which represents the initial level of *in vivo* fibrosis and the reference point for each animal. Statistical analysis was done with these normalized data. Statistical comparisons for significance between each time point were made using the non-parametric Mann–Whitney test. In each model, time points were compared two × two. The level of significance was set at $P < 0.05$. Results were expressed as means ± SEM.

3. Results

3.1. Extracellular matrix organization in rat PCLS

In normal liver, Sirius red staining was essentially observed in centrolobular vein wall and in portal connective tissue; in CCl_4-treated animals, fibrotic lesions were classically observed around centrolobular veins and in thin septa between centrolobular zones; after bile duct ligation, proliferation of bile structures was typically accompanied by extracellular matrix deposition (data not shown).

In cultured PCLS derived from both CCl_4-treated and bile duct ligated animals, there were no obvious modifications of the Sirius red staining. However, the organisation of the Sirius red stained material which clearly surrounded the ductular structures in non-cultured PCLS derived from bile duct ligated animals was, after culture, slightly modified following the remodelling of the ductular structures (see below) which induced a slackening of the Sirius red stained fibers around these structures (data not shown). By immunohistochemistry, no modifications of the collagen type I and III expression were observed in cultured PCLS compared with non-cultured PCLS (data not shown). Gelatin zymography revealed that, in PCLS derived from both CCl_4-treated and bile duct ligated animals, pro-MMP-2 slightly decreased during culture while the active MMP-2 greatly increased (Fig. 1). Pro-MMP-9 decreased in cultured PCLS derived from both CCl_4-treated and bile duct ligated animals compared with non-cultured PCLS; active MMP-9 was present only in non-cultured PCLS derived from bile duct ligated animals and was undetectable after culture (Fig. 1).

3.2. Modification of the myofibroblastic phenotype in rat PCLS

In normal liver, as previously described, α-SM actin was present only in walls of centrolobular veins and of portal tract vessels [25]; PDGF receptor-β expression was limited to centrolobular veins, to portal vessels, and to a few mesenchymal cells of the portal tract stroma [11] (data not shown).

After CCl_4 treatment, before culture, a strong expression of α-SM actin (Fig. 2a) and of PDGF receptor-β

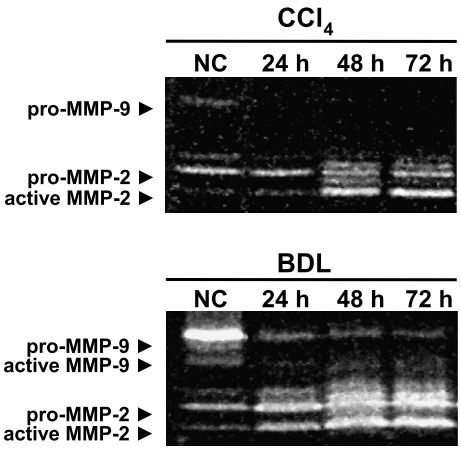

Fig. 1. Expression of MMP-2 and MMP-9 measured in gelatin-containing gels by zymography. A band migrating at 66 kDa corresponding to pro-MMP-2 and a 62-kDa band corresponding to active MMP-2 are detected; compared with non-cultured (NC) PCLS, an important increase of the active MMP-2 is observed in cultured PCLS derived from both CCl_4-treated and bile duct ligated (BDL) animals. Regarding MMP-9, a band migrating at 95 kDa and corresponding to pro-MMP-9 is detected; compared with non-cultured PCLS, a decrease is observed in cultured PCLS derived from both CCl_4-treated animals and bile duct ligated animals; active MMP-9 is only barely detectable in non-cultured PCLS derived from bile duct ligated animals, and is undetectable after culture. The experiment was repeated several times with identical results. One representative experiment is shown.

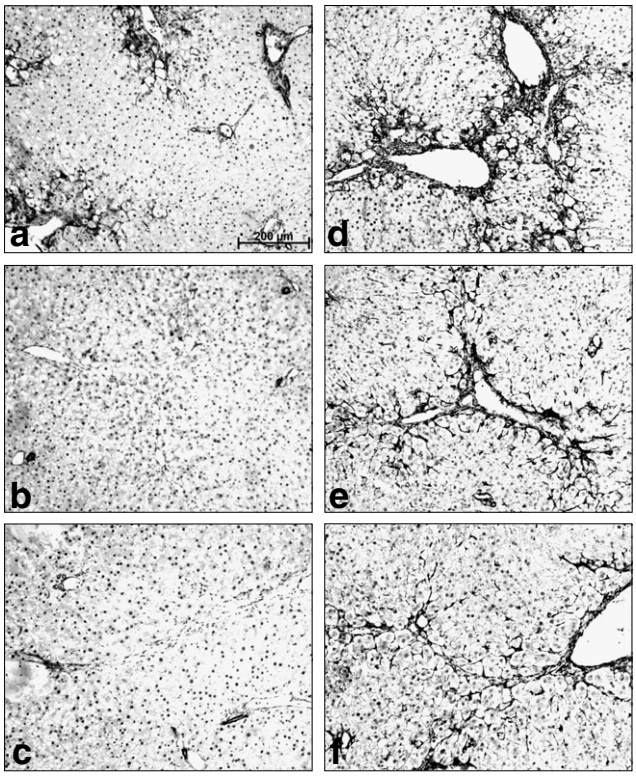

Fig. 2. α-SM actin (a–c) and PDGF receptor-β (d–f) expression in PCLS derived from CCl_4-treated animals, non-cultured (a, d), or cultured for 24 (b, e) or 48 h (c, f). Before culture, numerous myofibroblastic cells around centrolobular veins express both α-SM actin (a) and PDGF receptor-β (d); PDGF receptor-β staining concerns more cells compared with α-SM actin staining. After 24 h in culture, only vessels express α-SM actin (b) while PDGF receptor-β expression is not modified (e). After 48 h in culture, α-SM actin expression is no more modified (c), while PDGF receptor-β expression decreases (f).

(Fig. 2d) was observed in numerous myofibroblastic cells around centrolobular veins; indeed, PDGF receptor-β staining was more extended compared with α-SM actin staining. After 24 h in culture, α-SM actin expression was clearly decreased (Fig. 2b) while PDGF receptor-β expression was only slightly but not significantly modified (Fig. 2e). After 48 h in culture, α-SM actin expression was almost absent, except in vessel walls (Fig. 2c), while PDGF receptor-β expression significantly decreased (Fig. 2f). Quantitative image analysis showed the early disappearance of α-SM actin expression while PDGF receptor expression progressively decreased with a slight expression maintained even after 72 h in culture (Fig. 3).

After bile duct ligation, before culture, α-SM actin (Fig. 4a) and PDGF receptor-β (Fig. 4d) expression was obvious in enlarged portal tracts around proliferating bile ductules. After 24 h in culture, α-SM actin (Fig. 4b) and PDGF receptor-β (Fig. 4e) expression was not significantly modified. After 48 h in culture, both α-SM actin (Fig. 4c) and PDGF receptor-β (Fig. 4f) expression was strongly decreased. Quantitative

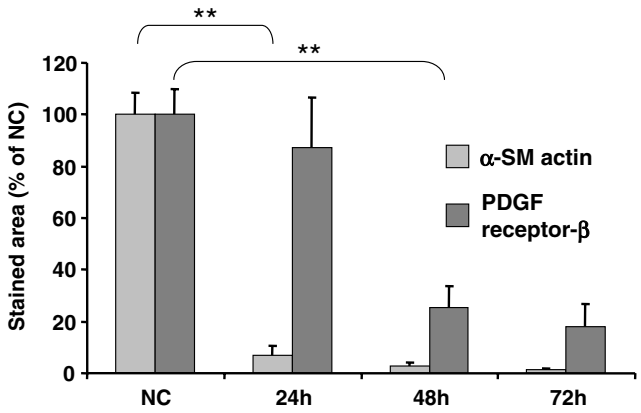

Fig. 3. Quantitative image analysis of α-SM actin and of PDGF receptor-β expression in PCLS derived from CCl_4-treated animals, non-cultured, or cultured for 24, 48, or 72 h. Compared with non-cultured PCLS, α-SM actin expression is drastically reduced after 24 h in culture (6.97; $P < 0.01$); PDGF receptor-β expression is significantly reduced only after 48 h in culture (25.52; $P < 0.01$).

image analysis showed no modifications of α-SM actin and of PDGF receptor-β expression after 24 h in culture, but a parallel decrease of both myofibroblast activation markers after 48 h in culture (Fig. 5).

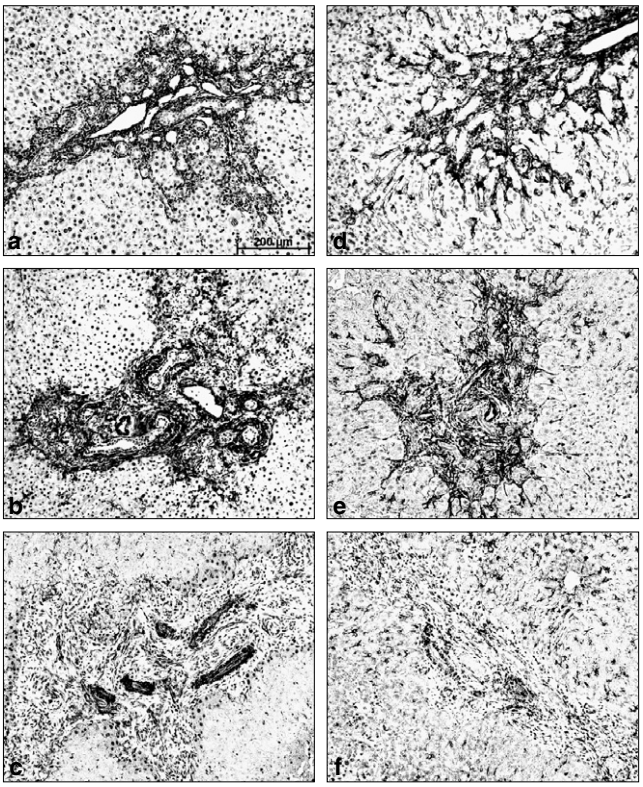

Fig. 4. α-SM actin (a–c) and PDGF receptor-β (d–f) expression in PCLS derived from bile duct ligated animals, non-cultured (a,d), or cultured for 24 (b e) or 48 h (c,f). In non-cultured PCLS, a strong expression of α-SM actin (a) and of PDGF receptor-β (d) is observed in numerous myofibroblastic cells present around proliferating bile ductules. After 24 h in culture, the expression of both α-SM actin (b) and of PDGF receptor-β (e) is not modified. After 48 h in culture, both α-SM actin (c) and PDGF receptor-β (f) expression drastically decrease.

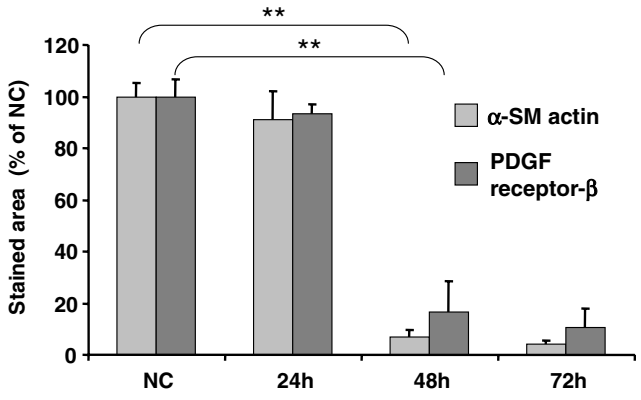

Fig. 5. Quantitative image analysis of α-SM actin and of PDGF receptor-β expression in PCLS derived from bile duct ligated animals, non-cultured, or cultured for 24, 48, or 72 h. Compared with non-cultured PCLS, α-SM actin and PDGF receptor-β expression are significantly reduced after 48 h in culture (7.05 and 16.72, respectively; $P < 0.01$).

3.3. Fibrogenic cell behaviour in rat PCLS

In normal liver, no apoptotic active caspase 3 positive cells were observed. After CCl_4 treatment, before culture, rare active caspase 3 positive hepatocytes were observed (Fig. 6a). After 6 h (Fig. 6b), 24 h (Fig. 6c), 48 h or 72 h (data not shown) in culture, no apoptotic cells were observed in PCLS derived from CCl_4-treated animals.

After bile duct ligation, before culture (Fig. 6d), and after 24 h in culture (data not shown), only a few active caspase 3 positive hepatocytes were observed around portal zones. But after 48 h in culture, numerous apoptotic cells, including (myo) fibroblasts and biliary epithelial cells, were detected in portal zones (Fig. 6e); after 72 h in culture (Fig. 6f), among the remaining cells in portal zones, numerous were apoptotic. Fig. 6d–f clearly show the decrease of the cellularity in portal zones. No apoptotic sinusoidal cells were observed.

In PCLS derived from CCl_4-treated animals, before culture, vimentin staining allowed the detection of the mesenchymal cells involved in the development of the lesion around centrolobular veins (Fig. 7a); after 72 h in culture, numerous vimentin positive cells were always detected in the fibrotic lesions around centrolobular veins (Fig. 7b). In PCLS derived from bile duct ligated-animals, before culture, portal myofibroblasts and proliferating biliary epithelial cells expressed vimentin (Fig. 7c); after 72 h in culture, an important decrease of the vimentin expression was observed in portal zones (Fig. 7d); osteopontin expression was also decreased, underlining the disappearance of the biliary epithelial cells (data not shown); in contrast with the impressive remodelling observed in portal zones, the parenchyma

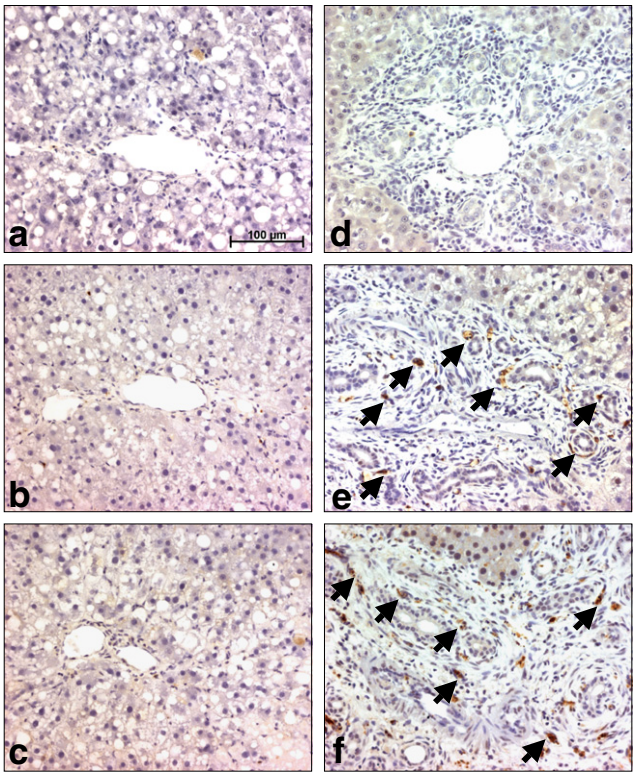

Fig. 6. Active caspase 3 expression in PCLS derived from CCl_4-treated animals non-cultured (a) or cultured for 6 h (b) or 24 h (c), or derived from bile duct ligated animals non-cultured (d), or cultured for 48 (e) or 72 h (f). In PCLS derived from CCl_4-treated animals, very rare apoptotic cells expressing active caspase 3 are detected in non-cultured (a) and cultured (b,c) PCLS. In PCLS derived from bile duct ligated animals, except very rare active caspase 3 expressing hepatocyte, no apoptotic cells are observed in non-cultured PCLS (d); in contrast, after 48 h (e) and 72 h (f) in culture, numerous active caspase 3 expressing cells are present in the portal lesions.

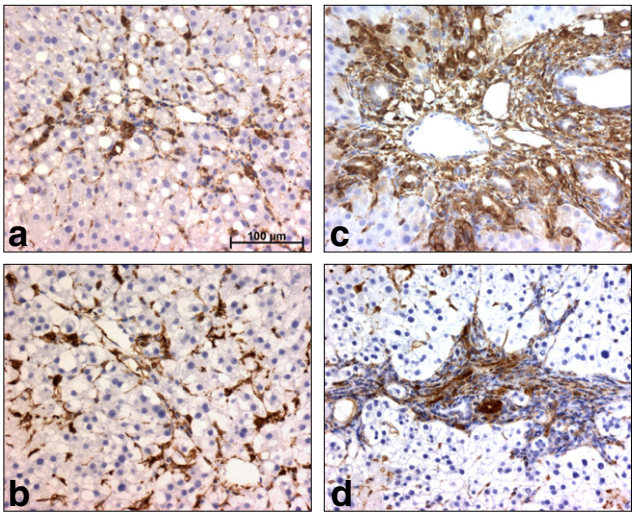

Fig. 7. Vimentin expression in PCLS derived from CCl_4-treated animals (a, b) or from bile duct ligated animals (c,d), non-cultured (a,c), or cultured for 72 h (b,d). In PCLS derived from CCl_4-treated animals, vimentin-positive cells are observed around centrolobular veins in non-cultured PCLS (a). After 72 h in culture vimentin expression is not modified (b). In PCLS derived from bile duct ligated animals, numerous vimentin positive cells, myofibroblasts and biliary epithelial cells, are observed (c). After 72 h in culture vimentin expression is dramatically reduced in portal tracts, only few positive cells are still observed (d).

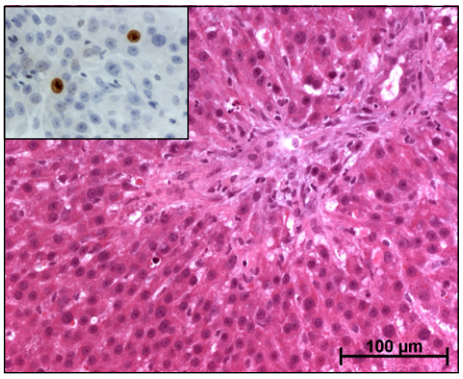

Fig. 8. Hematoxylin-eosin staining and Ki67 immunostaining (insert) in PCLS derived from bile duct ligated animals. After 72 h in culture, the parenchyma surrounding a remodelled portal region is well preserved; moreover, Ki67 expression demonstrates that a few hepatocytes proliferate.

was well preserved with a few hepatocytes in proliferation (Fig. 8).

3.4. Transmission electron microscopy observation of rat PCLS

In non-cultured PCLS derived from CCl_4-treated animals, numerous cells with typical features of myofibroblasts including bundles of microfilaments and indented nuclei were observed between the hepatocytes at the periphery of the lesions (Fig. 9a). In PCLS derived from CCl_4-treated animals and cultured for 48 h, fibroblastic cells without evident signs of activation were present in the Disse space between the sinusoidal lumen (S) and hepatocytes (H) (Fig. 9b); these cells were embedded in a loose collagen matrix (Fig. 9b and c) and some of them contained lipid droplets (Fig. 9c). In non-cultured PCLS derived from bile duct ligated animals, myofibroblastic cells embedded in a dense collagen matrix were present around ductular structures (Fig. 9d and e); after 24 h in culture, portal areas appeared disorganised and contained numerous apoptotic cells presenting typical chromatin condensation (Fig. 9f).

3.5. Evolution of the human fibrotic lesions in cultured PCLS

The histology of the human liver specimens is given in Table 1. In non-cultured PCLS, numerous α-SM actin expressing myofibroblasts were present in septa of alcoholic cirrhosis (Fig. 10a) and surrounding numerous biliary structures in portal zones of cholestatic diseases (Fig. 10c). After 48 h in culture, whatever the aetiology, α-SM actin expression disappeared, except in vessels (Fig. 10b and d). In all human liver specimens, no obvious modifications of the parenchyma, as evaluated on hematoxylin-eosin-stained sections, were observed during PCLS culture.

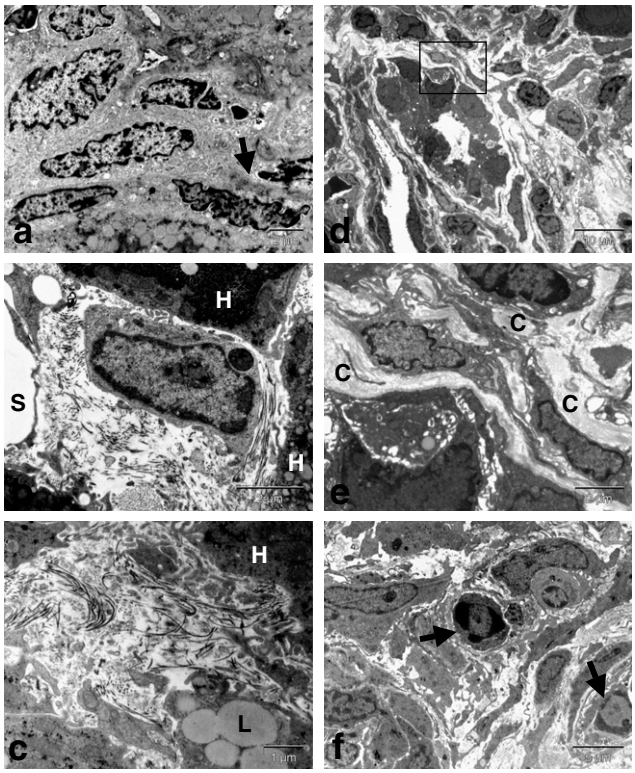

Fig. 9. Transmission electron microscopy of PCLS derived from CCl_4-treated animals (a–c) or from bile duct ligated animals (d–f), non-cultured (a,d,e), or cultured for 48 h (b,c,f). PCLS derived from CCl_4-treated animals: in non-cultured PCLS, numerous cells with typical features of myofibroblasts including bundles of microfilaments (arrows) and indented nuclei are observed; in PCLS cultured for 48 h (b,c), fibroblastic cells without evident signs of activation, sometimes containing cytoplasmic lipid droplets (L), and embedded in a loose collagen matrix are present in the Disse space between the sinusoidal lumen (S) and hepatocytes (H). PCLS derived from bile duct ligated animals: in non-cultured PCLS (d, e), myofibroblastic cells embedded in a dense collagen matrix (C) are present around ductular structures (e is an enlargement of the square box drawn in d); after 48 h in culture (f), apoptotic cells (arrows) with chromatin condensation are present in disorganised portal areas.

4. Discussion

In this study, two well-known experimental models were used to induce liver fibrosis in rats: CCl_4 model where hepatic stellate cells constitute the main fibrogenic cells involved, and bile duct ligation model which induces bile duct proliferation [26,27] and a rapid activation of portal fibroblasts [3,28]. When activated, both hepatic stellate cells and portal fibroblasts early express the PDGF receptor-β [18–20] and acquire a myofibroblastic phenotype characterized by the expression of α-SM actin [21]. Here, we show that, in PCLS derived from CCl_4-treated animals, α-SM actin expression disappeared early in culture while PDGF receptor-β expression progressively decreased; moreover, no obvious disappearance by apoptosis of the fibrogenic cells was observed (absence of active caspase 3 detection), and

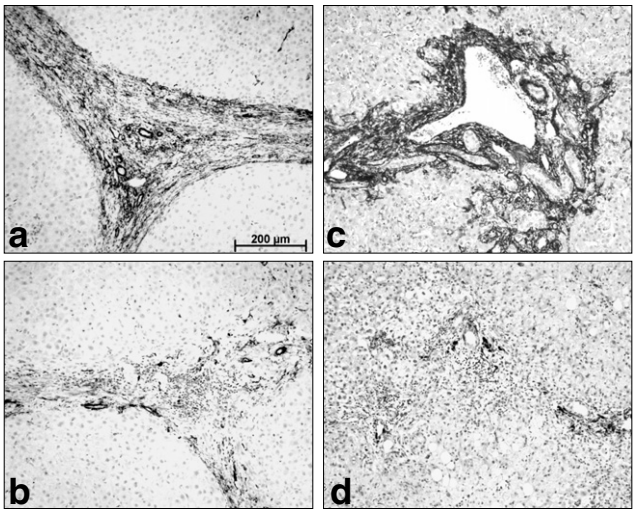

Fig. 10. α-SM actin expression in PCLS derived from cirrhotic (a, b) or cholestatic (c,d) human livers, non-cultured (a, c), or cultured for 48 h (b,d). In non-cultured PCLS, numerous myofibroblasts expressing α-SM actin are present in septa of cirrhotic liver (a) and in portal zones of fibrotic cholestatic liver (c); when PCLS are cultured for 48 h, a disappearance of α-SM actin expression is observed, excepted in vessel wall, in both cirrhotic (b) and fibrotic cholestatic (d) lesions.

numerous vimentin-positive cells were still observed in the lesion areas after 72 h in culture. In PCLS derived from bile duct ligated animals, α-SM actin and PDGF receptor-β decreased in parallel during PCLS culture, and in contrast with the observations obtained in cultured PCLS derived from CCl_4-treated animals, numerous active caspase 3 expressing apoptotic cells, including myofibroblasts and biliary epithelial cells, were detected in fibrotic areas; after culture for 72 h, the drastic decrease of vimentin expression in portal zones confirmed the disappearance of the vimentin expressing cells, i.e. myofibroblasts and proliferating biliary epithelial cells. These observations provide the evidence that fibrogenic cells involved in fibrogenesis which develops in these two models do not evolve similarly during the remodelling process occurring in cultured PCLS. So, we can hypothesize that the mechanisms leading to myofibroblastic differentiation and deactivation are different in these two models, and/or myofibroblastic cells involved in the development of the fibrotic lesions belong to different fibrogenic cell sub-populations with their own characteristics. In addition, these modifications concerning fibrogenic cell behaviour in cultured PCLS were observed in absence of obvious extracellular matrix alterations; however, active MMP-2 was increased during PCLS culture, while MMP-9 was decreased, showing that during PCLS culture, MMP expression and activity are regulated, probably participating in the early and subtle events affecting PCLS organisation.

Several groups have shown that activated hepatic stellate cells can revert to quiescence [29,30], suggesting that hepatic stellate cells have a plastic phenotype. In PCLS derived from CCl_4-treated animals, culture could induce at least in part a reversibility of the myofibroblastic phenotype. However, it has been shown that the lesion induced by CCl_4 treatment spontaneously regresses *in vivo*, with a disappearance of the activated hepatic stellate cells by apoptosis [31]. Interestingly, our results show that in PCLS culture, the myofibroblastic differentiation of the hepatic stellate cells is lost with an early disappearance of α-SM actin expression and a progressive decrease of PDGF receptor-β expression, but without induction of cell death by apoptosis; this underlines the importance of the cell environment in inducing different cell behaviour. Indeed, it has clearly been demonstrated that the stiffness of the surrounding environment determines the phenotype of multiple cell types [32], including hepatic stellate cells [33]. This could explain the differences observed during remodelling *in vivo* and in PCLS culture.

In the bile duct ligation model, it has been suggested that the increase of hydrostatic pressure in bile ducts induces biliary epithelial cell damage and bile duct proliferation [34] accompanied by a rapid activation of portal fibroblasts [3,28]. After bile duct ligation, it has been shown that mere biliary decompression by relieving the mechanical stress or bilioduodenal anastomosis induces apoptosis of portal cells, including portal myofibroblasts, that likely triggers portal fibrosis regression [35,36]. In PCLS derived from bile duct ligated animals, it is probable that the disappearance of the mechanical stress linked to bile duct ligation induces, similarly to what is observed *in vivo*, portal fibroblast apoptosis and portal lesion remodelling. This was confirmed by the fact that α-SM actin and PDGF receptor-β expression decreases together with the apparition of active caspase 3 expressing cells.

Our observations underline the diversity of the fibrogenic cells involved in experimental liver fibrogenesis, and the different fate of these cells during tissue remodelling induced in our model by culture conditions. These modifications were observed without any effects of the culture conditions on the viability of sinusoidal cells which do not express active caspase 3. In previous studies, it has also been shown that culture conditions do not affect the viability of sinusoidal cells and that this PCLS model is relevant to study the functions of hepatic stellate cells [10,37,38], endothelial cells [39] and Kupffer cells [40,41]. It has been shown that rat liver myofibroblasts derived from portal fibroblasts and hepatic stellate cells differ in CD95-mediated apoptosis and response to tumour necrosis factor-α [42]. Moreover, insulin-like growth factor-1 induces DNA synthesis and apoptosis in rat liver hepatic stellate cells but DNA synthesis and proliferation in rat liver myofibroblasts [43]. Together with our observations, these studies illustrate the diversity

of the fibrogenic cells involved in liver fibrogenesis, and show that the different fibrogenic cell populations share different mechanisms of activation and deactivation.

Moreover, in this study, PCLS were prepared using human cirrhotic and fibrotic cholestatic livers. In the two types of diseases, numerous α-SM actin expressing myofibroblasts were observed. During PCLS culture, a disappearance of the α-SM actin expression was observed in both cases. Obviously, further studies using more human samples are necessary, and the mechanisms involved in tissue remodelling of rat experimental lesions which develop in some days and of human fibrotic livers which result from an injury present for months to years are not comparable. However, these preliminary observations using human tissues confirm the relevance of this model to study the remodelling of fibrotic liver tissue according to the aetiology of the disease.

In conclusion, our study shows that rat liver fibrotic tissue is remodelled differently in cultured PCLS according to the aetiology of fibrosis; after CCl_4 treatment, a proportion of myofibroblasts derived from hepatic stellate cells seems to dedifferentiate while in the bile duct ligation model, myofibroblasts derived from portal fibroblasts disappear by apoptosis. We confirm here in the PCLS model previous data showing the different behaviour of the fibrogenic cells during liver remodelling and in addition, we demonstrate (1) that studies using PCLS could reduce number of animals necessary for studies on liver remodelling and (2) that PCLS may be a valuable tool to study the mechanisms of fibrogenesis and tissue repair in human liver samples.

Acknowledgements

This work was supported in part by Région Aquitaine. Christelle Guyot holds a fellowship from Région Aquitaine. We thank the staff of the Service Commun de Microscopie Electronique (SERCOMI, Université Victor Segalen Bordeaux 2, France) for performing transmission electron microscopy sample preparation. We are very grateful to Dr. Daniel Hartmann (Novotec, Lyon, France) for providing antibodies against collagens type I and III, and to Dr. Sylviane Guerret (Novotec) for technical support.

References

[1] Guyot C, Lepreux S, Combe C, Doudnikoff E, Bioulac-Sage P, Balabaud C, et al. Hepatic fibrosis and cirrhosis: the (myo)fibroblastic cell subpopulations involved. Int J Biochem Cell Biol 2006;38:135–151.

[2] Lotersztajn S, Julien B, Teixeira-Clerc F, Grenard P, Mallat A. Hepatic fibrosis: molecular mechanisms and drug targets. Annu Rev Pharmacol Toxicol 2005;45:605–628.

[3] Tuchweber B, Desmoulière A, Bochaton-Piallat ML, Rubbia-Brandt L, Gabbiani G. Proliferation and phenotypic modulation of portal fibroblasts in the early stages of cholestatic fibrosis in the rat. Lab Invest 1996;74:265–278.

[4] Benyon RC, Iredale JP. Is liver fibrosis reversible?. Gut 2000;46:443–446.

[5] Wanless IR, Nakashima E, Sherman M. Regression of human cirrhosis. Morphologic features and the genesis of incomplete septal cirrhosis. Arch Pathol Lab Med 2000;124:1599–1607.

[6] Desmet VJ, Roskams T. Cirrhosis reversal: a duel between dogma and myth. J Hepatol 2004;40:860–867.

[7] Lerche-Langrand C, Toutain HJ. Precision-cut liver slices: characteristics and use for *in vitro* pharmaco-toxicology. Toxicology 2000;153:221–253.

[8] Moronvalle-Halley V, Sacre-Salem B, Sallez V, Labbe G, Gautier JC. Evaluation of cultured, precision-cut rat liver slices as a model to study drug-induced liver apoptosis. Toxicology 2005;207:203–214.

[9] Vickers AE, Saulnier M, Cruz E, Merema MT, Rose K, Bentley P, et al. Organ slice viability extended for pathway characterization: an *in vitro* model to investigate fibrosis. Toxicol Sci 2004;82:534–544.

[10] van de Bovenkamp M, Groothuis GM, Draaisma AL, Merema MT, Bezuijen JI, van Gils MJ, et al. Precision-cut liver slices as a new model to study toxicity-induced hepatic stellate cell activation in a physiologic milieu. Toxicol Sci 2005;85:632–638.

[11] Clouzeau-Girard H, Guyot C, Combe C, Moronvalle-Halley V, Housset C, Rosenbaum J, et al. Effects of bile acids on biliary epithelial cell proliferation and portal fibroblast activation using rat liver slices. Lab Invest 2006;86:275–285.

[12] Dubuisson L, Desmoulière A, Decourt B, Evade L, Bedin C, Boussarie L, et al. Inhibition of liver fibrogenesis through noradrenergic antagonism. Hepatology 2002;35:325–331.

[13] Taras D, Blanc JF, Rullier A, Dugot-Senant N, Laurendeau I, Bièche I, et al. Halofuginone suppresses the lung metastasis of chemically induced hepatocellular carcinoma in rats through MMP inhibition. Neoplasia 2006;8:312–318.

[14] Vialle-Presles MJ, Hartmann DJ, Franc S, Herbage D. Immunohistochemical study of the biological fate of a subcutaneous bovine collagen implant in rat. Histochemistry. 1989;91:177–184.

[15] Skalli O, Ropraz P, Trzeciak A, Benzonana G, Gillessen D, Gabbiani G. A monoclonal antibody against alpha-smooth muscle actin: a new probe for smooth muscle differentiation. J Cell Biol 1986;103:2787–2796.

[16] Haft CR, de la Luz Sierra M, Barr VA, Haft DH, Taylor SI. Identification of a family of sorting nexin molecules and characterization of their association with receptors. Mol Cell Biol 1998;18:7278–7287.

[17] Alves da Costa C, Mattson MP, Ancolio K, Checler F. The C-terminal fragment of presenilin 2 triggers p53-mediated staurosporine-induced apoptosis, a function independent of the presenilinase-derived N-terminal counterpart. J Biol Chem 2003;278:12064–12069.

[18] Pinzani M, Milani S, Grappone C, Weber Jr FL, Gentilini P, Abboud HE. Expression of platelet-derived growth factor in a model of acute liver injury. Hepatology 1994;19:701–707.

[19] Wong L, Yamasaki G, Johnson RJ, Friedman SL. Induction of beta-platelet-derived growth factor receptor in rat hepatic lipocytes during cellular activation *in vivo* and in culture. J Clin Invest 1994;94:1563–1569.

[20] Pinzani M, Milani S, Herbst H, DeFranco R, Grappone C, Gentilini A, et al. Expression of platelet-derived growth factor and its receptors in normal human liver and during active hepatic fibrogenesis. Am J Pathol 1996;148:785–800.

[21] Tomasek JJ, Gabbiani G, Hinz B, Chaponnier C, Brown RA. Myofibroblasts and mechano-regulation of connective tissue remodelling. Nat Rev Mol Cell Biol 2002;3:349–363.

[22] Omary MB, Coulombe PA, McLean WH. Intermediate filament proteins and their associated diseases. N Engl J Med 2004;351:2087–2100.
[23] Nakanuma Y, Kono N. Expression of vimentin in proliferating and damaged bile ductules and interlobular bile ducts in nonneoplastic hepatobiliary diseases. Mod Pathol 1992;5:550–554.
[24] Lorena D, Darby I, Gadeau AP, Lam Shang Leen L, Rittling S, Porto LC, et al. Osteopontin expression in normal and fibrotic liver. Altered liver healing in osteopontin-deficient mice. J Hepatol 2006;44:383–390.
[25] Uchio K, Tuchweber B, Manabe N, Gabbiani G, Rosenbaum J, Desmoulière A. Cellular retinol-binding protein-1 expression and modulation during *in vivo* and *in vitro* myofibroblastic differentiation of rat hepatic stellate cells and portal fibroblasts. Lab Invest 2002;82:619–628.
[26] Alpini G, Lenzi R, Sarkozi L, Tavoloni N. Biliary physiology in rats with bile ductular cell hyperplasia. Evidence for a secretory function of proliferated bile ductules. J Clin Invest 1988;81:569–578.
[27] Marucci L, Baroni GS, Mancini R, Benedetti A, Jezequel AM, Orlandi F. Cell proliferation following extrahepatic biliary obstruction. Evaluation by immunohistochemical methods. J Hepatol 1993;17:163–169.
[28] Desmoulière A, Darby I, Monte Alto Costa A, Raccurt M, Tuchweber B, Sommer P, et al. Extracellular matrix deposition, lysyl oxydase expression, and myofibroblastic differentiation during the initial stages of cholestatic fibrosis in the rat. Lab Invest 1997;76:765–778.
[29] Sohara N, Znoyko I, Levy MT, Trojanowska M, Reuben A. Reversal of activation of human myofibroblast-like cells by culture on a basement membrane-like substrate. J Hepatol 2002;37:214–221.
[30] Gaca MD, Zhou X, Issa R, Kiriella K, Iredale JP, Benyon RC. Basement membrane-like matrix inhibits proliferation and collagen synthesis by activated rat hepatic stellate cells: evidence for matrix-dependent deactivation of stellate cells. Matrix Biol 2003;22:229–239.
[31] Iredale JP, Benyon RC, Pickering J, McCullen M, Northrop M, Pawley S, et al. Mechanisms of spontaneous resolution of rat liver fibrosis. Hepatic stellate cell apoptosis and reduced hepatic expression of metalloproteinase inhibitors. J Clin Invest 1998;102:538–549.
[32] Yeung T, Georges PC, Flanagan LA, Marg B, Ortiz M, Funaki M, et al. Effects of substrate stiffness on cell morphology, cytoskeletal structure, and adhesion. Cell Motil Cytoskeleton 2005;60:24–34.
[33] Wells RG. The role of matrix stiffness in hepatic stellate cell activation and liver fibrosis. J Clin Gastroenterol 2005;39:158–161.
[34] Slott PA, Liu MH, Tavoloni N. Origin, pattern, and mechanism of bile duct proliferation following biliary obstruction in the rat. Gastroenterology 1990;99:466–477.
[35] Ramm GA, Carr SC, Bridle KR, Li L, Britton RS, Crawford DH, et al. Morphology of liver repair following cholestatic liver injury: resolution of ductal hyperplasia, matrix deposition and regression of myofibroblasts. Liver 2000;20:387–396.
[36] Costa AM, Tuchweber B, Lamireau T, Yousef IM, Balabaud C, Rosenbaum J, et al. Role of apoptosis in the remodeling of cholestatic liver injury following release of the mechanical stress. Virchows Arch 2003;442:372–380.
[37] Vickers AE, Saulnier M, Cruz E, Merema MT, Rose K, Bentley P, et al. Organ slice viability extended for pathway characterization: an *in vitro* model to investigate fibrosis. Toxicol Sci 2004;82:534–544.
[38] M. van de Bovenkamp, G.M. Groothuis, D.K. Meijer, P. Olinga, Precision-cut fibrotic rat liver slices as a new model to test the effects of anti-fibrotic drugs *in vitro*, J Hepatol (in press).
[39] Olinga P, Hof IH, Merema MT, Smit M, de Jager MH, Swart PJ, et al. The applicability of rat and human liver slices to the study of mechanisms of hepatic drug uptake. J Pharmacol Toxicol Methods 2001;45:55–63.
[40] Neyrinck AM, Taper HS, Gevers V, Declerck B, Delzenne NM. Inhibition of Kupffer cell activity induces hepatic triglyceride synthesis in fasted rats, independent of lipopolysaccharide challenge. J Hepatol 2002;36:466–473.
[41] Olinga P, Merema MT, de Jager MH, Derks F, Melgert BN, Moshage H, et al. Rat liver slices as a tool to study LPS-induced inflammatory response in the liver. J Hepatol 2001;35:187–194.
[42] Saile B, Matthes N, Neubauer K, Eisenbach C, El-Armouche H, Dudas J, et al. Rat liver myofibroblasts and hepatic stellate cells differ in CD95-mediated apoptosis and response to TNF-alpha. Am J Physiol Gastroint Liver Physiol 2002;283:G435–G444.
[43] Saile B, DiRocco P, Dudas J, El-Armouche H, Sebb H, Eisenbach C, et al. IGF-I induces DNA synthesis and apoptosis in rat liver hepatic stellate cells (HSC) but DNA synthesis and proliferation in rat liver myofibroblasts (rMF). Lab Invest 2004;84:1037–1049.